Electro-refraction in standard and symmetrically coupled Ge/SiGe quantum wells

Jacopo Frigerio*[a], Vladylav Vakarin[b], Papichaya Chaisakul[b], Andrea Ballabio[a], Daniel Chrastina[a], Marco Leone[a], Xavier Le Roux[b], Laurent Vivien[b], Giovanni Isella[a] and Delphine Marris-Morini[b]

[a]L-NESS, Dipartimento di Fisica del Politecnico di Milano, Polo di Como, Via Anzani 42, 22100 Como, Italy
[b] Centre de Nanosciences et de nanotechnologies, Université Paris Sud, CNRS, Université Paris Saclay, 91405 Orsay, France

* jacopo.frigerio@polimi.it,

Submitted: 01/12/2016 Accepted: 24/03/2017

ABSTRACT

Electro-refraction in standard (sQW) and coupled (cQW) Ge/SiGe quantum wells grown on Si have been investigated by means of optical transmission measurements performed on planar waveguides. The anomalous Quantum confined Stark Effect observed in the coupled quantum well structure strongly enhance the electro-refractive effect with respect to sQW.

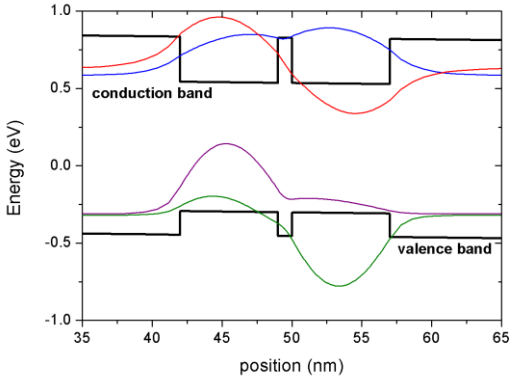

Keywords: Germanium, quantum wells, silicon photonics, modulators

In the last decade, optical devices based on Ge/SiGe quantum wells deposited on Si have undergone an impressive development driven by the envisioned applications in silicon photonics. The strong quantum confined Stark effect (QCSE) observed in this material system[1], has opened a path toward the realization of compact and efficient optical modulators. Intensity modulation at 1490[2-3-4] nm and at 1550[5-6] nm has been demonstrated in different exciting works, as well as high-speed operation[2]. Thanks to their compactness, Ge/SiGe QW modulators can reach power consumption levels as low as 10 fJ/bit[2], thus meeting the very aggressive requirements for on-chip optical interconnects[7].Composition and thicknesses of Ge/SiGe MQW can be finely tailored in order to engineer the material bandgap and to consequently address a very wide range of modulation wavelengths. This approach has been exploited to demonstrate intensity modulation at 1300 nm by increasing the compressive strain in the Ge layers in Ge/$Si_{0.35}Ge_{0.65}$ grown on a $Si_{0.3}Ge_{0.7}$ buffer [8-9-10] or simply by reducing the well thickness in Ge/$Si_{0.15}Ge_{0.85}$ MQW[11]. All the aforementioned modulators work by exploiting QCSE of the first excitonic transition (cΓ1-HH1),

nevertheless, also the second excitonic transition (cΓ1-LH1) was investigated[12]. Recently, an integrated optical link made by a Ge/SiGe MQW modulator and photodetector connected through a low- loss SiGe waveguide was demonstrated[13]. Remarkably, all the devices were monolithically integrated on silicon by a single epitaxial growth. This work has stimulated the study of SiGe as a new material platform for silicon photonics and several fundamental components of the passive optical circuitry has been demonstrated[14]. An excellent review of optical modulators based on Ge/SiGe MQW can be found in[15]. Ge/SiGe quantum wells have also been successfully employed to realize other silicon compatible integrated optical components such as inter-band[16] and inter-subband[17] photodetectors and light emitting diodes[18,19]. QCSE causes strong variations in the absorption spectrum, leading to a significant change of the effective index as stated by Kramers-Kronig relations, thus the QCSE can be used to realize efficient phase modulators. In this work, we compare the electro-refractive effect in Ge/SiGe standard (sQW) and symmetrically coupled (cQW) Ge/SiGe quantum wells deposited on silicon. The heterostructures were grown by Low Energy Plasma enhanced chemical vapor deposition (LEPECVD)[20] on 100 mm n-Si(001) substrates with a resistivity of 1-10 Ω cm. Before the heteroepitaxial growth, the substrates were dipped in an aqueous hydrofluoric acid solution for 30 seconds to remove the native oxide. The first part of the structure consists for both samples of a $Si_{1-y}Ge_y$ graded buffer, with a total thickness of 13 μm, where the Ge concentration y was linearly raised from 0% to 90% with a grading rate of 7%/μm. The growth rate was 5-10 nm/s, while the substrate temperature was linearly decreased from 740°C to 525°C. The graded buffer was then capped with a 2 μm thick p-doped ($5x10^{18}$ cm^{-3}) $Si_{0.1}Ge_{0.9}$ layer to form a fully relaxed virtual substrate (VS) and the p-type contact of the p-i-n structure embedding the heterostructures. The threading dislocation density was 6 x 10^6 cm^2 as measured by chemical defect etching. The sQW consists of 20 repetitions of the following structure (10 nm Ge well + 15 nm $Si_{0.15}Ge_{0.85}$ barrier) while the cQW consists of seven repetitions of the following structure (10 nm Ge well + 3 nm $Si_{0.15}Ge_{0.85}$ inner barrier + 10 nm Ge well + 37 nm $Si_{0.15}Ge_{0.85}$ outer barrier). The thickness of the QW region is similar for both the samples. The quantum well stacks were grown at 475°C at a rate of 1 nm/s. Individual layer thicknesses and compositions were designed to realize a strain-symmetrized structures. Finally a 200 nm phosphorous doped (1 x 10^{19} cm^{-3}) $Si_{0.1}Ge_{0.9}$ n-type contact layer was deposited for both the samples. A cross section of the structures is shown in Fig. 1.

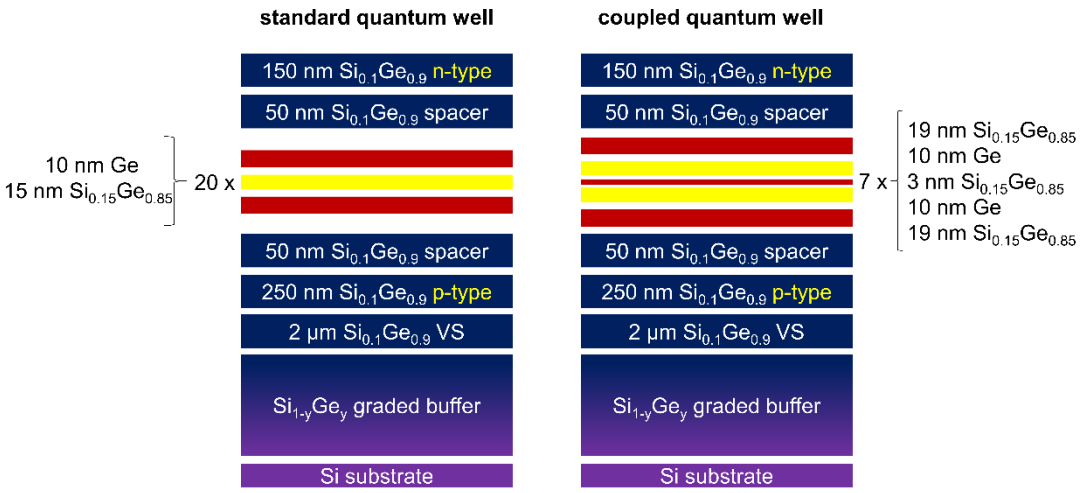

Figure 1: Schematic of the sample with detailed growth steps.

Layer compositions and strain states were measured by high-resolution x-ray diffraction (HR-XRD) by using a PANalytical X'Pert PRO MRD diffractometer. Out-of-plane and in-plane lattice parameters, were measured (relative to the Si reflection) for the VS peak and the superlattice satellites. Ge content and strain were then obtained using the known lattice parameters for relaxed SiGe alloys[21] and interpolated elastic constants of Si and Ge[22]. The final composition of the VS for both the samples was found to be 90.6% (with a residual in-plane strain of 0.05%). The in-plane lattice parameter of the MQW stack is the same as that of the VS for sQW and cQW, meaning that the heterostructure stacks are coherently matched to the VS. From the reciprocal space maps (see Fig. 2) it can be noticed that the diffraction peaks from the VS and the heterostructures are broadened perpendicular to the relaxation line (the line which joins the Bragg peak to the origin of reciprocal space) due to the mosaicity in the VS. The good crystalline quality of the samples can be inferred by the high number of satellite peaks that are visible in the reciprocal space maps.

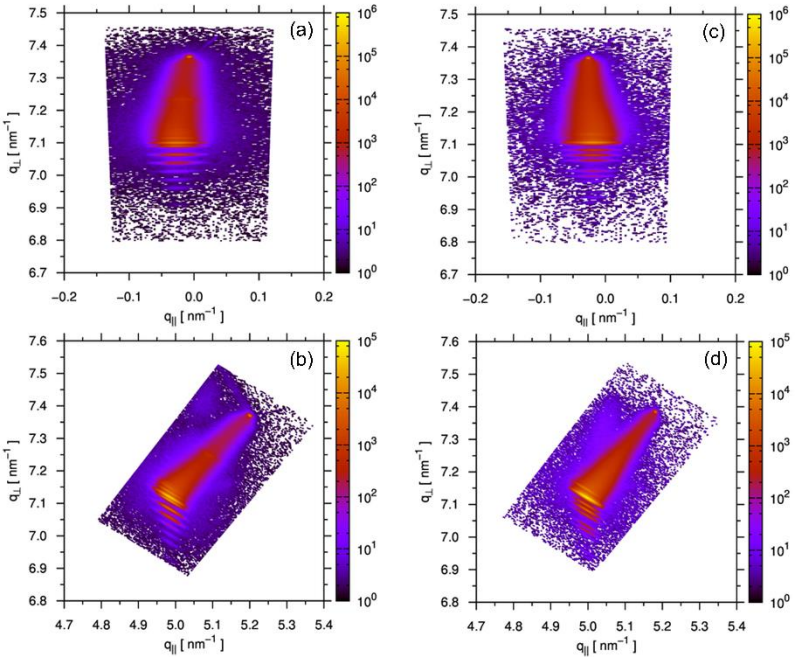

Figure 2: Reciprocal space maps of the sQW (a and b) and of the cQW (c and d) with respect to the 224 Si reflection and to the 004 Si reflection.

In order to investigate the electro-refractive effect in Ge/SiGe standard and coupled QWs, 64 μm long, 100 μm wide planar waveguides have been processed. The waveguides were patterned by optical lithography and then dry etched to the p-doped Si0.1Ge0.9 layer. The sidewall roughness of the etched mesa was smoothened by hydrogen peroxide (H2O2) solution. 100 nm of silicon dioxide were deposited as passivation layer on the left and right walls of the waveguide by plasma-enhanced chemical vapor deposition (PECVD). For n and p contacts 10 nm of Ti and 300 nm of Au was evaporated and lifted off. The measurements have been performed at room temperature with a spectral resolution of 0.1 nm. A tunable laser emitting light from 1250 to 1450 nm with a power of 1 mW has been used. Light from the laser has been butt coupled into the planar waveguide using a taper-lensed fiber, which has been positioned to inject light in the waveguide region not covered by the top metal contact to reduce optical losses. An objective has been used to couple the output light into a photodetector. The etched facets of the waveguides are partially reflective, thus a Fabry-Perot (FP) cavity is formed within the waveguide. As a consequence, the absorption spectra of the heterostructures are modulated by FP fringes. The effective index variation can be deduced by measuring the spectral shift of the FP fringes as a function of the electric field applied to the heterostructures. The detailed procedure can be found in[23,24].

The effective index variation as a function of different applied electric fields for sQW and cQW is reported in figure 3 a and b respectively.

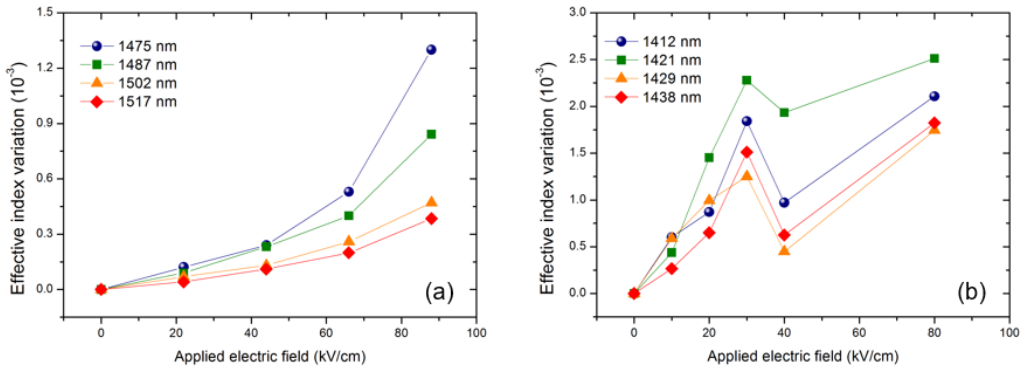

Figure 3: Effective index variation as a function of the applied electric field at different wavelengths for sQW (a) and cQW (b).

For standard quantum wells, the effective index variation increases with the applied electric field and decreases as we move away from the main excitonic transition. Such a behaviour is perfectly consistent with QCSE. An effective index variation up to 1.3×10^{-3} is measured at 1475 nm (see fig. 3a) with an applied electric field of 88 kV/cm, which corresponds to an applied bias voltage of 8V, with an associated $V_\pi L_\pi$ figure of merit of 0.46 V cm. This value is comparable to those reported for III-V standard quantum wells[25,26] and competitive with those of silicon[27]. In the case of cQW the effective index variation has a local maximum for all the considered wavelengths at 30 kV/cm and it is not monotonically decreasing at increasing wavelength. An effective index variation of 2.3×10^{-3} is obtained for 30 kV/cm (1.5 V) at 1421 nm (see fig. 3b), with an associated $V_\pi L_\pi$ figure of merit of 0.045 Vcm. This value is one order of magnitude higher with respect to sQW. In the case of sQW, the absorption spectra at different applied electric fields show a clear QCSE (see fig. 4a). By increasing the electric field, the excitonic peak shifts towards longer wavelengths and the intensity is progressively reduced. In the case of cQW, we can observe two peaks, which are very close in energy. By increasing the electric field, the intensity of the absorption peak at longer wavelength progressively increases, while the intensity of the other peak is decreasing (see fig. 4 b). The enhanced electro-refractive effect observed in the cQW structure arises from two main spectral features. First of all there is a huge absorption variation at an intermediate electric field (30 kV/cm for this structure) which causes the presence of a local maximum in the effective index variation as a function of the electric field. On the contrary, for the sQW there is only a monotonic increase of the effective index with increasing electric field. Moreover, the two main absorption peaks in the cQW do not shift in energy as the electric

field increases, allowing the exploitation of the electro-refractive effect closer to the excitonic resonances without high losses. This is not possible in sQW because the excitonic peak shift toward longer wavelengths as the electric field increases. A detailed explanation of the QCSE in cQW can be found in[28].

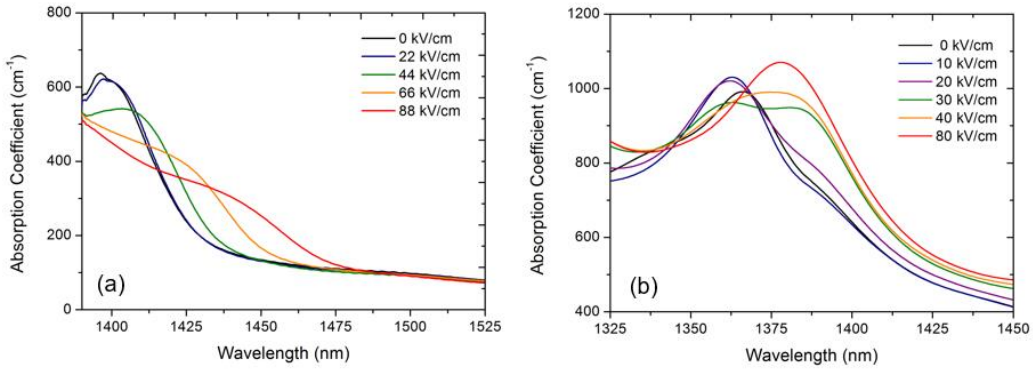

Figure 4: Smoothed absorption spectra for different applied electric fields for sQW (a) and cQW (b).

To summarize, we have investigated the electro-refraction in Ge/SiGe standard and symmetrically coupled quantum wells. The cQW shows an enhanced electro-refractive effect with an effective index variation higher than $2x10^{-3}$ under a moderate electric field. In order to exploit the potentiality of Ge/SiGe CQW as compact, high speed and low power consumption optical modulators, the active region will have to be integrated into an interferometric structure such as a Mach– Zehnder interferometer. The integration of QW active regions with low-loss SiGe waveguides on top of graded buffer is a promising approach, as sharp bends and Mach-Zehnder interferometers[14] as well as the integration of a passive SiGe waveguide with an electro-absorption modulator and a photodetector[13] were demonstrated recently.

ACKNOWLEDGEMENT

The fabrication of the device was performed at the nano-center CTU-IEF-Minerve, which is partially funded by the 'Conseil General de l'Essonne'. This work was partly supported by the French RENATECH network. D.M-M. acknowledges support by the Institut Universitaire de France. Marie Curie International Outgoing Fellowships through grant agreement PIOF-GA-2013-629292 MIDEX is partly acknowledged.This project has received funding from the European Research Council (ERC) under the European Union's Horizon 2020 research and innovation programme (grant agreement N°639107-INsPIRE).

References

[1] Y.H. Kuo, Y. Lee, Y. Ge, S. Ren, J.E. Roth, T.I. Kaminis, D.A.B. Miller, and J.S. Harris. Nature 437, 1334 (2005).

[2] P. Chaisakul, D. Marris-Morini, M.S. Roufied, G. Isella, D. Chrastina, J. Frigerio , X. Le Roux, S. Edmond, J.R. Coudevylle and L Vivien, Opt. Express 20, 3219 (2012).

[3] S. Ren , Y. Rong , T.I. Kaminis, J.S. Harris and D.A.B. Miller, Appl. Phys. Lett. 98, 151108 (2011).

[4] S. Ren ,Y. Rong, S.A. Claussen, R.K. Schaevitz, T.I. Kaminis, J.S. Harris and D.A.B. Miller, IEEE Photon. Tech. Lett. 24, 461 (2012).

[5] Y.H. Kuo, Y.K. Lee, Y. Ge, S. Ren, J.E. Roth, T.I. Kamins, D.A.B. Miller and J.S. Harris, IEEE J. Sel. Top. Quantum Electron. 12, 1503 (2006).

[6] D.C.S Dumas, K. Gallacher, S. Rhead, M. Myronov, D.R. Leadley and D.J. Paul, Optics Express 22, 19284 (2014).

[7] D.A.B. Miller, Opt. Express 20, A293 (2012).

[8] L. Lever, Y. Hu, M. Myronov, X. Liu, N. Owens, F.Y. Gardes, I.P. Marko, S.J. Sweeney, Z. Ikonić, D.R. Leadley, G.T. Reed and R.W. Kelsall, Opt. Lett. 36, 4158 (2011).

[9] M.S. Rouifed, P. Chaisakul, D. Marris-Morini, J. Frigerio, G. Isella, D. Chrastina, S. Edmond, X. Le Roux, J.R. Coudevylle and L Vivien, Opt. Lett. 37, 3960 (2012).

[10] M.S Rouifed, D. Marris-Morini, P. Chaisakul, J. Frigerio, G. Isella, D. Chrastina, S. Edmond, X. Le Roux, J.R. Coudevylle ,D. Bouville and L. Vivien, IEEE J. of Sel. Top. In Quantum Elect. 20, 33-(2014).

[11] P. Chaisakul, J. Frigerio, D. Marris-Morini, V. Vakarin, D. Chrastina, G. Isella and L. Vivien L., J. Appl. Phys. 116, 193103 (2014).

[12] P. Chaisakul, D. Marris-Morini, M.S. Rouifed, J. Frigerio, G. Isella, D. Chrastina, J.R. Coudevylle, X. Le Roux, S. Edmond, D. Bouville and L. Vivien, Appl. Phys. Lett. 102, 191107 (2013).

[13] P. Chaisakul, D. Marris-Morini, J. Frigerio, D. Chrastina, M.S. Rouifed, S. Cecchi, P. Crozat, G. Isella and L. Vivien,
Nat. Photon. 8, 482 (2014).

[14] V. Vakarin, P. Chaisakul, J. Frigerio, A. Ballabio, X. Le Roux, J.R.Coudevylle, D. Bouville, D. Perez-Galacho, L. Vivien, G. Isella and D. Marris-Morini, Opt. Express 23, 30821 (2015).

[15] P. Chaisakul, D. Marris-Morini, M.S. Rouifed, J. Frigerio, D. Chrastina, J.R. Coudevylle, X. Le Roux, S. Edmond, G. Isella and L. Vivien, Sci. Tech. Adv. Mat. 15, 014601 (2014).

[16] P. Chaisakul, D. Marris-Morini, G. Isella, D. Chrastina, M.S. Rouifed, X. Le Roux, S. Edmond, E. Cassan, J. R. Coudevylle, and L. Vivien, IEEE Phot. Tech. Lett. 23, 1430 (2011).

[17] K. Gallacher, A. Ballabio, R.W. Millar, J. Frigerio, A. Bashir, I. MacLaren, G .Isella, M. Ortolani, D.J. Paul, Appl. Phys. Lett. 108, 091114 (2016).

[18] K. Gallacher, P. Velha, D.J. Paul, S. Cecchi, J. Frigerio, D. Chrastina and G. Isella, Appl. Phys Lett. 101, 211101 (2012).

[19] P. Chaisakul, D. Marris-Morini, G. Isella, D. Chrastina, N. Izard, X. Le Roux, S. Edmond, J.R. Coudevylle, L. Vivien, Appl. Phys. Lett 99 141106 (2011).

[20] G. Isella , D.Chrastina, B. Rössner, T. Hackbarth, H.J. Herzog , U. König, and H. von Känel, Solid State Electron. 48, 1317 (2004).

[21] J.P. Dismukes, L. Ekstrom and R.J. Paff, J. Phys. Chem. 68, 3021 (1964).

[22] J.J. Wortman and R.A. Evans, J. Appl. Phys. 36, 153 (1965).

[23] J. Frigerio, P. Chaisakul, D. Marris-Morini, S. Cecchi, M.S. Roufied, D. Chrastina, G. Isella and L. Vivien, Appl. Phys. Lett. 102, 061102 (2013).

[24] J. Frigerio, P. Chaisakul, D. Marris-Morini, S. Cecchi, M.S. Roufied, G. Isella and L. Vivien, SPIE Microtechnologies. 87670B (2013).

[25] J. S. Wiener, D. A. B. Miller, and D. S. Chemla, Appl. Phys. Lett. 50, 842 (1987).
[26] L. Glick, F. K. Reinhart, G. Weimann, and W. Schlapp, Appl. Phys. Lett. 48, 989 (1986).

[27] M.J.W. Green, M.J. Rooks, L. Sekaric and Y.A. Vlasov, Opt. Express 15, 17106 (2007).

[28] J. Frigerio, V. Vakarin, P. Chaisakul, M. Ferretto, D. Chrastina, X. Le Roux, L. Vivien, G. Isella and D. Marris-Morini D., Scientific Reports 5, 15398 (2015).